

for $H \gg M_0$, i. e., when the external magnetic field is much greater than the local fields of the crystal.

At $k \neq 0$, the calculation of the integral in (12) becomes complicated, with the exception of the case $k \ll k_{11m}$, when it is not difficult to obtain the following expression for $\gamma_{3c}(k)$:

$$\gamma_{3c}(k) = \gamma_{3c}(0) + \gamma_1 a^2 k^2, \quad \gamma_1 \sim \frac{M_0^2}{T_c} \left(\frac{T_c}{T} \right)^{3/2} \left(\frac{T}{H} \right)^{1/2} \quad (16)$$

Estimate of k_{11m} from the relation (14) for YIG at room temperature and $H \sim 10^3$ Oe gives $k_{11m} \sim 10^4$ cm⁻¹. This value lies on the lower boundary of this region of k , which has been studied experimentally up to the present time,^[2,3] which makes difficult the comparison of the obtained results with experiment. We note that the estimate $\gamma_{3c}(0)$ from the relation (14) gives $\gamma_{3c}(0) \sim 10^{-2}$ Oe for YIG at room temperature, which can be a significant fraction of the total line width of the better samples.^[2] It is also possible that the experimentally observed^[3] deviation from the expected linear law for the dependence of $\gamma(0)$ on T is connected with the contribution of the three-magnon coalescence processes considered in the work (according to (14), the contribution from such processes to $\gamma(0)$ changes with temperature as $T^{11/6} \sim T^2$).

In conclusion, it is a pleasure for the authors to

thank M. I. Kaganov, B. N. Provotorov and Yu. G. Rudyi for valuable comments. The authors are grateful to V. G. Bar'yakhtar and the theoretical group of the Donetsk Physico-technical Institute of the Ukrainian Academy of Sciences for interest in the work and useful discussions.

¹Analytic continuation is carried out by the standard method; see, for example, Ref. 8.

¹A. I. Akhiezer, V. G. Bar'yakhtar and S. V. Peletminskii, *Spinovye volny (Spin waves)* Nauka, 1967 [Pergamon, 1971].

²A. G. Gurevich, *Magnitnyi rezonans v ferritakh i antiferromagnetikakh (Magnetic resonance in ferrites and antiferromagnetics)* Nauka, 1973.

³A. G. Gurevich and A. N. Anisimov, *Zh. Eksp. Teor. Fiz.* **68**, 677 (1975) [Soviet Phys. JETP **41**, 336 (1975)].

⁴R. Peierls, *Quantum Theory of Solids (Russian translation, IL, 1956)*.

⁵A. A. Abrikosov, L. P. Gor'kov and I. E. Dzyaloshinskii, *Metody kvantovoi teorii polya v statisticheskoi fizike (Quantum Field Theoretical Methods in Statistical Physics)* Fizmatgiz, 1968 [Pergamon].

⁶J. Shy-Yih Wang, *Phys. Rev.* **B6**, 1908 (1972).

⁷V. L. Ginzburg and M. I. Kaganov, *Fiz. Tverd. Tela.* **10**, 3293 (1968) [Soviet Phys. Solid State **10**, 2603 (1969)].

⁸T. Holstein, *Annals of Phys.* **29**, 410 (1964).

⁹S. Simons, *Proc. Phys. Soc. (London)* **82**, 401 (1963).

¹⁰R. White and M. Sparks, *Phys. Rev.* **130**, 632 (1963).

Translated by R. T. Beyer

The resistive state and pinning in deformed single crystals of niobium

L. Ya. Vinnikov, V. I. Grigor'ev, and O. V. Zharikov

Institute of Solid State Physics, USSR Academy of Sciences

(Submitted July 21, 1975)

Zh. Eksp. Teor. Fiz. **71**, 252-261 (July 1976)

The current-voltage characteristics, pinning, and dislocation structure in deformed single crystals of niobium are studied. An effect of plastic deformation on the current-voltage characteristics near the upper critical field H_{c2} is observed. The observed features of the resistive state, the effect of deformation on the current-voltage characteristics, and the peak effect are discussed in terms of models that account for the possibility of varying the number of moving vortices and for the increase in the dynamic pinning force near H_{c2} in materials with an inhomogeneous distribution of pinning centers.

PACS numbers: 74.40.Gt

I. INTRODUCTION

The study of the resistive state, consisting of the current-voltage characteristics of type-II superconductors in the mixed state, yields the most complete information on pinning and on the motion of the vortex lattice. In most studies of type-II superconductors the current-voltage characteristics, observed while varying the external magnetic field H , are a series of curves with an initial nonlinear portion, becoming linear with further increase of the current. The slope of the linear portion is proportional to the magnetic field.^[1,2]

Since the reports by Kim and coworkers were pub-

lished^[1,2] it has been assumed that changes in the structural state of the superconductor (its imperfection or inhomogeneity) do not affect the shape of current-voltage characteristics, causing only their parallel shift along the current axis.^[1,2] An unusual behavior, however, of the current-voltage characteristics (near H_{c2} , at least) was observed in a number of studies, for example, in deformed Nb-Ti and Nb-Ta alloys,^[3-5] and in recrystallized foils of an Nb-Zr alloy.^[6] We have recently reported^[7] features of the current-voltage characteristics in stress-deformed single crystals of niobium near H_{c2} .

The present work is devoted to the features of the

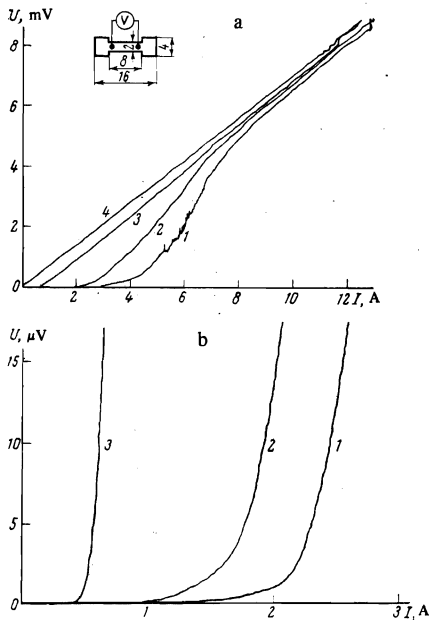


FIG. 1. Effect of plastic deformation on the current-voltage characteristics for $h=0.96$: a) CVC of samples: 1) deformed by rolling by 10%, 2) by 5%, 3) nondeformed samples, 4) in the normal state; b) low voltage current-voltage characteristics (for the same samples).

resistive state and of pinning in deformed niobium. The effect of plastic deformation on the current-voltage characteristics in various fields is investigated. The observed effects are compared with inhomogeneities in the dislocation structure and are discussed from the point of view of assuming a varying number of moving vortices^[8] and an increase in dynamic pinning near H_{c2} ^[9-11].

2. SAMPLES AND EXPERIMENTAL PROCEDURE

Plane samples 1.5 mm thick for deformation prepared by electric spark cutting from a single crystal niobium bar ($\varnothing 16 \times 200$ mm) melted by an electron beam from NVCh (highest-purity) material with a resistance ratio $R_{300K}/R_{4.2K} \approx 20$ at 6 kOe along the $\langle 110 \rangle$ direction of the bar axis. After grinding and removing the chemically polished cold-worked layer with the reagent consisting of a mixture of fluoric and nitric acids, stock pieces of thickness ~ 1 mm were deformed by rolling with a total compression 5–50%, or by 1.5–10% elongation with a strain rate 0.005 cm/min. The wide surface of the stock corresponded to the (001) plane, and served as the rolling plane in the $[110]$ direction. The elongation was also along $[110]$. After deformation the samples were cut from the stock along the $\langle 110 \rangle$ direction, and were used for electrical measurements after chemical thinning to a thickness 0.2 mm. The sizes, shape, and distance (in mm) between the potential contacts are shown in Fig. 1a. The current and potential contacts were soldered with indium solder to the samples, which were tinned beforehand with an ultrasonic soldering iron. The current-voltage characteristics were recorded with PDS-021 or PDP4-002 automatic x - y recorders at a scanning ratio 2 A/min, up to various voltage levels on the samples, through which transport cur-

rent I was passed. The measurements were performed in a transverse magnetic field, perpendicular to the (001) plane, at a temperature $T=4.2$ K, and in several cases at $T=1.9$ K, i. e., in superfluid helium. H_{c2} was determined by linear extrapolation of the steeply decreasing portion of the $J_c(H)$ curve to $J_c=0$ ($H_{c2}=4700$ Oe), where J_c is the critical current density corresponding to the appearance of a voltage $U=10^{-7}$ V across the sample.

The foils for the electron microscopy were prepared in a mixture of lactic, sulfuric, and fluoric acids according to a method earlier described,^[12] both from the deformed stock pieces and from the samples following the electric measurements. The study of the crystal dislocation structure was carried out with a JEM-150 electron microscope with an accelerating voltage 150 kV.

3. MEASUREMENT RESULTS

Figure 2 shows current-voltage characteristics corresponding to different relative magnetic fields $h=H/H_{c2}$ applied to a sample deformed by rolling down to $\epsilon=10\%$. The current-voltage characteristics were recorded up to the highest possible voltages, until thermal destruction of the resistive state (the thermal transition is denoted by a vertical mark on the figure; after the transition the sample resistance is close to normal). The field dependence of the current-voltage characteristics is conveniently described by means of several relative-field values h_1 and h_p .

The current-voltage characteristics can be divided into two groups: I) current-voltage characteristics with no singularities, similar to those described in^[1,2] and observed at $h < h_1$ ($h_1 \approx 0.8$ at a strain deformation $\epsilon=10\%$); II) current-voltage characteristics with singularities at $h > h_1$. The current-voltage characteristics of the second kind are characterized by the following features, established by recording them at various scales. In the initial nonlinear section ($U \leq 10^{-3}$ V) the differential resistance $R_d = dU/dI$ at constant voltage decreases, and the length of this section increases with an anoma-

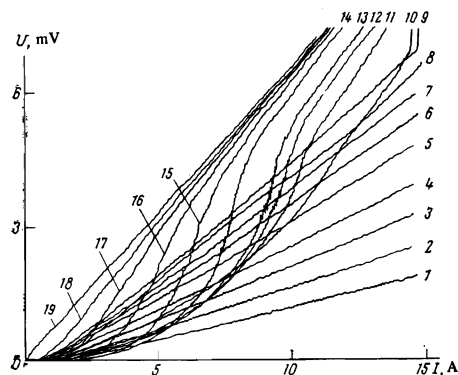


FIG. 2. Current-voltage characteristics for a sample deformed by rolling by 10% in various relative magnetic fields. Group I (curves 1–9): 1) $h=0.28$; 2) 0.36; 3) 0.44; 4) 0.52; 5) 0.60; 6) 0.67; 7) 0.71; 8) 0.78; 9) 0.83. Group II (curves 10–18): 10) $h=0.915$; 11) 0.92; 12) 0.93; 13) 0.05; 14) 0.96; 15) 0.97; 16) 0.98; 17) 0.99; 18) 0.995. Curve 19 is for $h=1.3$.

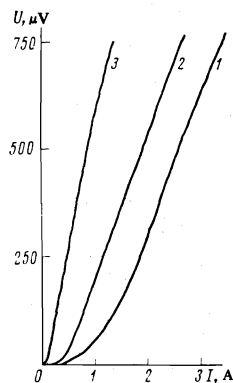


FIG. 3. Effect of plastic deformation on the current-voltage characteristics at $h=0.63$ for samples deformed by rolling by 10% (curve 2) and 30% (curve 1). Curve 3 corresponds to the current-voltage characteristics of samples in the normal state.

lously small slope for fields increasing up to $h=h_p$, where the effect is maximal ($h_p=0.96$ at a strain $\epsilon=10\%$). Further, at $h_p < h < 1$ this effect gradually decreases. In the interval $10^{-9} \text{ V} < U < 10^{-3} \text{ V}$ the location of h_p is independent of voltage. At higher voltages ($U > 10^{-3} \text{ V}$) the current-voltage characteristics have sections with $R_d > R_n$ (R_n is the sample resistance in the normal state), as earlier noted by us.^[7] Unlike the assumption made by us,^[7] however, the current-voltage characteristics nowhere become linear with a slope corresponding to Kim's empirical law,^[1,2] but gradually approach the straight line corresponding to R_n .

The values of h_1 and h_p depend on the method and degree of sample deformation: h_1 and h_p decrease with increasing plastic deformation. Thus, for example, for rolling-induced strains ϵ equal to 10, 30, and 50% the h_p values are 0.96, 0.94, and 0.90, respectively, and the h_1 values are ≈ 0.8 , ≈ 0.75 , and ≈ 0.6 , respectively. The h_p and h_1 values vary appreciably at strains $\epsilon > 10\%$.

The effect of plastic deformation on current-voltage characteristics in strong relative fields, $h > h_1$, is illustrated in Fig. 1a. The slope of curve 4 ($h=1.3$) corresponds practically to R_n , which was identical for all three samples due to the equality of the geometric sizes, of the distances between the potential contacts, and of the resistivity in the normal state ρ_n . In the nondeformed sample the singularities of the current-voltage characteristics near H_{c2} are quite weakly pronounced, with deviations from the usual behavior of current-voltage characteristics increasing with enhanced deformation: the slopes of the initial sections (approximately up to $U \approx 5 \cdot 10^{-4} \text{ V}$) decrease, and the lengths of these sections increase with an anomalously low slope. To study the initial sections, the current-voltage characteristics were recorded in large scale (up to $U \approx 15 \cdot 10^{-6} \text{ V}$, Fig. 2b): it is seen that even at the lowest voltages the current-voltage characteristics have the same singularities. In samples elongated 2–10% these features were much more weakly pronounced at comparable strains; the effect, however, also increases with increasing strain.

The effect of plastic deformation on the current-voltage characteristics in small weak relative fields, $h < h_1$, is illustrated in Fig. 3. It is seen that at $\epsilon=30\%$ the initial nonlinear section is longer. It is noted, however, that the slope of the initial nonlinear section is not

anomalous, i. e., it increases with the field (for a given U) unlike its behavior in the interval of relative fields $h_1 < h < h_p$. At $\epsilon < 10\%$ the strain causes a small shift of the current-voltage characteristics along the current axis, with no significant change in the shape of the initial section.

Curves showing the magnetic field dependence of the critical current density, constructed for various voltage levels ($U=4 \cdot 10^{-9} - 10^{-6} \text{ V}$), show a peak effect in the range of fields where singularities appear on the current-voltage characteristics, i. e., at $h > h_1$. The peak height decreases with lowering the level of voltage recording. Figure 4 describes the behavior of $J_c(H)$ for various amounts of deformation. The peak height increases with enhanced plastic deformation, undergoing a broadening, and the position of the maximum is shifted toward lower fields. We point out that the peak maximum is reached in the relative field h_p corresponding to maximum length of the anomalous nonlinear section, and the initial rise of the curves $J_c(H)$ corresponds to the field h_1 , since $J_c(H)$ represent a section of the field dependence of the current-voltage characteristics at a fixed voltage level. Thus, the shape and position of the peak of $J_c(H)$ reflect the singularities of the current-voltage characteristics near H_{c2} with enhancement of plastic deformation.

The determination of the linear section of current-voltage characteristics of deformed samples is difficult, as seen from Figs. 1 and 2, because of the great length of the initial nonlinear section. On the other hand, at high-power dissipation, deviations of the current-voltage characteristics from linearity are possible because of sample heating.^[13] In relative fields $h < h_1$ the linear sections of the current-voltage characteristics could be separated. The initial deviation of current-voltage characteristics from linearity in these fields has made it possible to determine experimentally the power at which the effect of sample heating becomes noticeable.

A higher sample temperature at a fixed external magnetic field causes an increase in the relative field $h=H/H_{c2}(T)$, and, consequently, a change in the slope of the current-voltage characteristic and in its shift along the current axis. A thermal calculation, similar to that performed by Goncharov *et al.*,^[13] has shown that the experimentally observed deviations of the current-voltage characteristics from linearity at powers $10^{-3} - 10^{-2}$

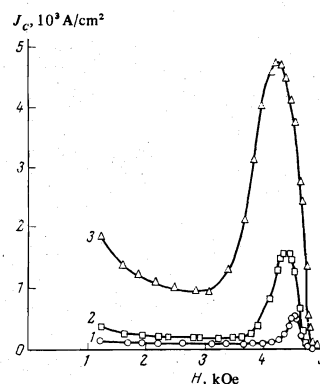


FIG. 4. Dependence of the critical current density J_c on the magnetic field H at voltage $U=10^{-7} \text{ V}$ for samples deformed by rolling: 1) $\epsilon=10\%$; 2) 30%; 3) 50%.

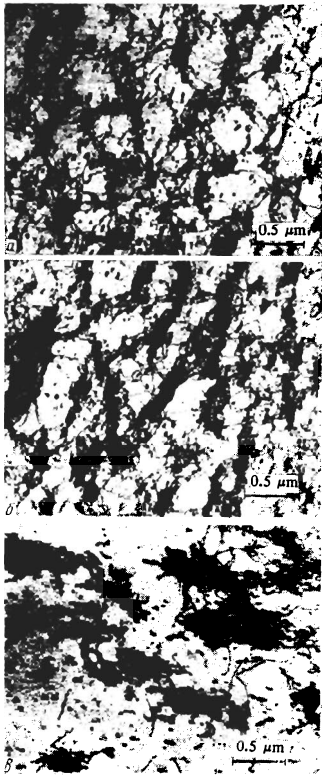


FIG. 5. Dislocation structure of samples deformed by rolling: a) $\epsilon = 5\%$, b) $\epsilon = 10\%$, and by stretching: c) $\epsilon = 3.5\%$. The foil plane is (001).

W in weak fields, $h < h_1$, can be attributed to overheating of the sample. In fields $h > h_1$ and powers $\sim 10^{-3}$ W sample overheating leads to a more complicated shape of the current-voltage characteristic, owing to the nonmonotonic nature of the h -dependence of J_c and of the slope of the initial nonlinear section. Therefore, in following discussions of the experimental results we restrict ourselves to those regions of the current-voltage characteristics, where sample overheating can be neglected. We point out that the variation in the viscosity coefficient $\eta(T)$ can be neglected at $T = 4.2$ K and at a maximum overheating $\Delta T \leq 0.3$ K.^[14]

The singularities on the current-voltage characteristics can also be caused by changes in the heat transfer from the sample to liquid helium. These singularities should disappear in superfluid helium.^[13] The current-voltage characteristic at 1.9 K showed that all observed singularities were qualitatively retained, i. e., they were not caused by changes in the nature of boiling of the helium. Oscillations on the steepest slopes of the current-voltage characteristics, which were noticeably pronounced at 4.2 K for strongly deformed samples, have, however, not been observed.

4. DISLOCATION STRUCTURE OF THE DEFORMED SAMPLES

To study the distributions of pinning centers (dislocations) introduced by the deformation, the sample structure was investigated by transmission electron microscopy. In the original undeformed samples of single-crystal Nb the dislocation density was $\approx 10^7$ cm⁻². The dislocation structure of samples, deformed by rolling by 5 and 10%, are shown in Figs. 5a and 5b, respective-

ly. The dislocations are nonuniformly distributed and are primarily grouped into interlacings that form the so-called cell structure, which is more strongly pronounced at larger degrees of deformation. Dislocation loops and dipoles are also observed in the cells, with distances of the order of several hundred Å between dislocations of opposite sign. The dislocation density in the interlacings (the cell walls) is higher by an order of magnitude than inside the cells. The total dislocation density after rolling deformation by 5 and 10% consisted of $(0.8 \pm 0.2) \cdot 10^{10}$ cm⁻² and $(2.5 \pm 0.7) \cdot 10^{10}$ cm⁻², respectively.

The size distribution of the cells is close to normal and, for example, for a rolling strain $\epsilon = 10\%$ it is characterized by an average cell radius of 0.3 μ m and an average square deviation of 0.1 μ m. When the rolling deformation is increased to $\epsilon = 30\%$ the dislocation density increases, mostly in the cell walls, but the cell sizes do not change considerably.

The dislocation structure of a sample deformed by stretching by 3.5%, is shown in Fig. 5c. Here the dislocations are extended, do not form closed cells, and are spaced ~ 1 μ m apart. With increasing deformation (up to 10%) the dislocation density in the interlacings increases also.

5. DISCUSSION

At the present time there does not exist a theory describing the resistive state of a type-II superconductor with pinning centers. The available phenomenological models either have no general experimental verification^[15,17] or are difficult to compare with experiment^[16]; therefore we discuss the results obtained on the basis of qualitative considerations.

Comparison of the current-voltage characteristics of the original and deformed samples (Figs. 1–3) shows the existence of a deformation effect on current-voltage characteristics, which can be due to the formation and change in the dislocation structure. Thus, for identical dislocation densities $\approx 7 \cdot 10^9$ cm⁻² (Figs. 5a, c) changes in the current-voltage characteristics are more strongly expressed for the cell structure, formed after rolling ($\epsilon = 5\%$), than for interlacing dislocations, formed by stretching ($\epsilon = 3.5\%$). With increasing deformation the dislocation density in the cell walls of rolled samples increases, as well as the deviation from the shape of a current-voltage characteristic of undeformed samples and J_c , which is more strongly pronounced near H_{c2} , increase. We assume that the dislocation structure, formed by deformation, is due to the type and distribution of pinning centers.

Comparison of the current-voltage characteristics of the original and variously deformed samples and analysis of their dislocation structure leads to the conclusion that the shapes and lengths of the initial nonlinear sections are determined by the type, density, and distribution of the pinning centers. In other words, the nonlinearity of current-voltage characteristics reflects the distribution function of the pinning force in the sample.^[8] Within the framework of these ideas the nonlinearity of

current-voltage characteristics is explained by the increasing number of moving vortices that break away from the pinning centers, and by the increasing Lorentz force accompanying the enhanced transport current. This means plastic flow of parts of the vortex lattice, or of individual vortex filaments separated from others, and pinned more tightly. For the simple distribution function of the pinning force, suggested in^[6]:

$$f(J) = \frac{1}{J_0} \exp\left(-\frac{J-J_c}{J_0}\right) \text{ for } J \geq J_c,$$

$$f(J) = 0 \text{ for } J < J_c,$$

where J_0 is the distribution parameter corresponding to the intercept of the current-density axis with the tangent to the point of the current-voltage characteristic (with a slope $R_{d \max}$) at the maximum value of J , the dependence of the function $\log(1 - R_d/R_{d \max})$ on J should be linear. The reduction of current-voltage characteristics (Fig. 6) shows that this function is more complicated, depends on the relative field, and changes near H_{c2} , at least for the deformed sample. This can be interpreted as a change in the pinning force distribution as a function of h . We point out that changing the shape of the current-voltage characteristics by introducing controllable pinning centers (dislocations) is a stronger argument for using these concepts concerning the nature of motion of lattice vortices than the agreement of any definite distribution function of the pinning forces, as suggested by other authors.^[8, 17-19]

The change in the pinning force-distribution with increasing h indicates a change in the interaction of the vortex lattice with the pinning centers close to H_{c2} . The possibility of the latter is discussed in connection with explaining the reason for the peak effect on the $J_c(H)$ curves.^[20] The $J_c(H)$ dependence reflects, as already shown (see Sec. 3 and^[7]), the behavior of current-voltage characteristics near H_{c2} . It is, therefore, expedient to discuss the peak effect and the features of current-voltage characteristics on the basis of concepts concerning the mechanism whereby the pinning centers are overcome.^[11, 20]

According to Kramer,^[11] the peak effect is due to an enhanced interaction of the vortex lattice with the pinning centers when its elastic properties change with increasing h : for centers of the same type of "point" interac-

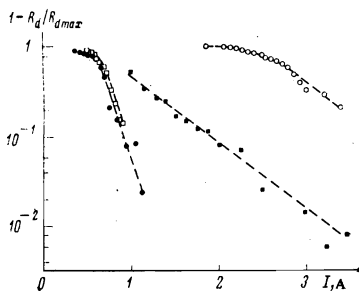


FIG. 6. Dependence of $\log(1 - R_d/R_{d \max})$ on the current I . \square —original sample, $h=0.96$; \blacksquare —original sample, $h=0.52$; \circ —sample deformed by rolling, $\epsilon=10\%$, $h=0.96$; \bullet —sample deformed by rolling, $\epsilon=10\%$, $h=0.55$.

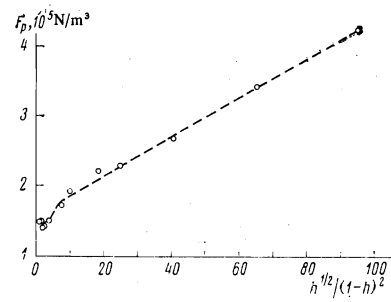


FIG. 7. Dependence of the pinning force density F_p on $h^{1/2}/(1-h)^2$ for samples deformed by rolling ($\epsilon=10\%$).

tion gives way to a "linear" interaction. In the first case the pinning centers act as individual points, and in the second case as a linear force. A criterion of the nature of the interaction is the critical length $l^* = C_{44}\Phi_0/C_{66}B)^{1/2}$, where C_{44} and C_{66} are the elastic constants of vortex lattice,^[21] Φ_0 is the magnetic flux quantum, and B is the magnetic induction. The quantity l^* varies with h as $l^* = L_0 h^{1/2}/(1-h)^2$, where L_0 is a constant, equal to $0.27 \mu\text{m}$ for Nb,^[20] $l^* = 0.52 \mu\text{m}$ for $h=0.6$, and $l^* = 5.26 \mu\text{m}$ for $h=0.95$. Assuming that the cell walls are the main pinning centers,^[22] in samples deformed by 10%, for example, the average cell diameter becomes smaller than l^* at $h > h^* = 0.6$, and in this case the interaction can be assumed linear. Besides, the dependence of the pinning force density F_p on $h^{1/2}/(1-h)^2$, where $F_p \approx J_c H$, undergoes a discontinuity at $h^{1/2}/(1-h)^2 \approx 4$ ($h \approx 0.6$), which according to Kramer and Osborne^[11, 20] also corresponds to a transition from a point to a line interaction (Fig. 7).

In relative fields $h > h^* \approx 0.6$, corresponding to the linear interaction, of the vortex lattice can adjust itself to the pinning centers, which can then become stronger, leading to an increase of F_p with h .^[11] A consequence of this can be a change in the pinning force distribution, which should change the shape, i. e., the lengths and slopes of the nonlinear sections of the current-voltage characteristics. An increase in the degree of plastic deformation increases the density of pinning centers and the effect itself.

In fields corresponding to the linear interaction, the function $F_p(h)$ calculated for various deformations (10, 30, 50%) has a maximum at $h = h_p$ and its value decreases with increasing deformation (Fig. 8). Such a behavior of $F_p(h)$ suggests a change in the mechanism of overcoming the pinning centers with increasing h .^[11] The vortex motion at $h < h_p$ occurs mostly by detachment, while for $h > h_p$ plastic vortex flow takes place relative to the pinning centers. Nevertheless, in fields $h < h_p$ plastic flow at a relatively high shear strength of the vortex lattice is possible either because of its local fluctuations^[20] or as a result of dipole and dislocation motion in the vortex lattice.^[23, 24] We point out that since near H_{c2} the shear strength of the vortex lattice is lowered by the decrease of the elastic constant $C_{66} \sim (1-h)^2$,^[21] the motion of weakly pinned vortices is facilitated, and this can explain the dependence of J_c on the recorded voltage level observed in other papers.^[5, 18]

Thus, the nonlinearity of the current-voltage charac-

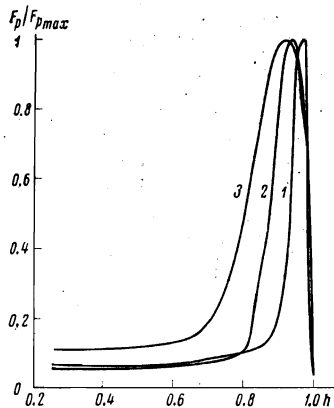


FIG. 8. Dependence of the reduced pinning force density F_p/F_{pmax} on h for samples deformed by rolling: 1) $\epsilon=10\%$, 2) $\epsilon=30\%$, 3) $\epsilon=50\%$.

teristics can be understood on the basis of concepts of plastic flow of the vortex lattice, and reflects the interaction of the vortices with the pinning centers.

6. DISCUSSION

An effect of plastic deformation of niobium single crystals on the shape of current-voltage characteristics has been established: a change in the extent of the initial nonlinear portion and the appearance of initial nonlinear portions with anomalously small slopes near H_{c2} have been detected. It was shown that the nonlinearity of the current-voltage characteristics and the pinning force depend on the type of structure, density, and distribution of the dislocations. With increasing dislocation density in the cell walls, the deviations near H_{c2} from the usual behavior of the current-voltage characteristics increase and, correspondingly, the peak of the $J_c(H)$ curve increases, and the position of its maximum is shifted towards the lower fields.

Thus, a correspondence has been shown between features of current-voltage characteristics and the peak behavior of the $J_c(H)$ curve, which agrees with the assumption that a transition from point to line pinning and an enhancement of the vortex interactions with the pinning centers take place near H_{c2} with increasing h . In this case the nonlinearity of the initial portions of current-voltage characteristics can be interpreted as a plastic flow of a vortex lattice. The complicated shapes of current-voltage characteristics near H_{c2} are, obvi-

ously, due to a simultaneous effect of deformation and sample heating at high dissipated-power values.

In conclusion the authors are grateful to V. V. Shmidt for reading the manuscript and for helpful remarks, to I. N. Goncharov, D. Frichevskii, K. K. Likharev, and V. A. Shukhman for discussing the results, and to Ch. V. Kopetskiĭ for his interest in this work.

- ¹A. R. Strand, C. F. Hempstead, and Y. B. Kim, *Phys. Rev. Lett.* **13**, 794 (1964).
- ²Y. B. Kim, C. F. Hempstead, and A. R. Strand, *Phys. Rev.* **139**, A1163 (1965).
- ³C. C. Chang and J. B. McKinnon, *Phys. Lett.* **27A**, 414 (1968).
- ⁴C. C. Chang, J. B. McKinnon, and A. C. Rose-Innes, *Phys. Stat. Solidi* **36**, 205 (1969).
- ⁵K. E. Osborne and A. C. Rose-Innes, *Phil. Mag.* **27**, 683 (1973).
- ⁶I. N. Gencharev and I. S. Khukharova, *Zh. Eksp. Teor. Fiz.* **62**, 627 (1972) [*Sov. Phys. JETP* **35**, 331 (1972)].
- ⁷L. Ya. Vinnikov and O. V. Zharikov, *Fiz. Tverd. Tela (Leningrad)* **16**, 3149 (1974) [*Sov. Phys. Solid State* **16**, 2042 (1975)].
- ⁸J. Baiexeras and G. Fournet, *J. Phys. Chem. Solids* **28**, 1541 (1967).
- ⁹A. B. Pippard, *Phil. Mag.* **19**, 217 (1969).
- ¹⁰J. A. Good and E. J. Kramer, *Phil. Mag.* **22**, 329 (1970).
- ¹¹E. J. Kramer, *J. Appl. Phys.* **44**, 1360 (1973).
- ¹²L. Ya. Vinnikov and A. A. Shul'ga, *Zev. Lab.* **39**, 981 (1973).
- ¹³I. N. Goncharev, G. L. Dorofeev, L. V. Petrava, and I. S. Khukhareva, *JINR Preprint R8-6260* (1972).
- ¹⁴I. N. Goncharev, G. L. Dorofeev, A. Nikitiu, L. V. Petrova, D. Frichevskii, and I. S. Khukhareva, *Zh. Eksp. Teor. Fiz.* **67**, 2235 (1974) [*Sov. Phys. JETP* **40**, 1109 (1975)].
- ¹⁵P. W. Anderson, *Phys. Rev. Lett.* **9**, 309 (1962).
- ¹⁶J. Lowell, *J. Phys.* **C3**, 712 (1970).
- ¹⁷W. R. Hudson and R. J. Jirberg, *Sol. St. Comm.* **7**, 499 (1969).
- ¹⁸J. M. A. Wade, *Phil. Mag.* **24**, 339 (1971).
- ¹⁹R. G. Jones, E. H. Rhoderick, and A. C. Rose-Innes, *Phys. Lett.* **24A**, 318 (1967).
- ²⁰K. E. Osborne, and E. J. Kramer, *Phil. Mag.* **29**, 685 (1974).
- ²¹R. Lebusch, *Phys. Stat. Sol.* **32**, 439 (1969).
- ²²A. V. Narlikar and D. Dew-Hughes, *Phys. Stat. Sol.* **6**, 338 (1964).
- ²³E. J. Kramer, *J. Appl. Phys.* **41**, 621 (1970).
- ²⁴M. I. Turchinskaya and A. L. Roĭburd, *Pis'ma Zh. Eksp. Teor. Fiz.* **20**, 185 (1974) [*JETP Lett.* **20**, 79 (1974)].

Translated by Nathan Jacobi